Front. Optoelectron. 2018, 11(3): 267–274
https://doi.org/10.1007/s12200-018-0829-6

RESEARCH ARTICLE

De-noising research on terahertz holographic reconstructed image based on weighted nuclear norm minimization method

Wenshu MA, Qi LI (✉), Jianye LU, Liyu SUN

National Key Laboratory of Science and Technology on Tunable Laser, Harbin Institute of Technology, Harbin 150080, China

Abstract Terahertz imaging is one of the forefront topics of imaging technology today. Denoising process is the key for improving the resolution of the terahertz holographic reconstructed image. Based on the fact that the weighted nuclear norm minimization (WNNM) method preserves the details of the reconstructed image well and the non-local mean (NLM) algorithm performs better in the removal of background noise, this paper proposes a new method in which the NLM algorithm is used to improve the WNNM method. The experimental observation and quantitative analysis of the denoising results prove that the new method has better denoising effect for the terahertz holographic reconstructed image.

Keywords terahertz digital holography, weighted nuclear norm minimization (WNNM), non-local mean (NLM)

1 Introduction

Terahertz imaging is one of the frontiers in imaging technology. Digital holographic imaging techniques have attracted great attention of the related researchers due to the special property about improving the image resolution [1,2]. In this paper, we use the terahertz Gabor in-line digital holography system proposed by our group, which is based on a CO_2 pumped 2.52 THz continuous-wave laser. When the collimated wave illuminates the object, the wave modulated by the object information is the object wave, and the rest of the transmitting wave is the reference wave. They interfere and form the interference pattern on the charge coupled device (CCD). As the imaging object is small and opaque, the high-resolution reconstruction of terahertz in-line digital holography is realized by an approximation operation in a construction process. Then use computer numerical calculation to achieve the reproduction process [3]. However, because of the presence of noise in imaging and acquisition process, it is necessary to denoise the reconstructed image to improve the resolution. The denoising methods for the terahertz holographic reconstructed image, such as non-local mean filtering, wavelet denoising [4,5].

Image denoising is the reverse solving process of obtaining the original image from the noise image. In recent years, with the development of mathematics, some new denoising methods have been proposed. At present, the low rank matrice problem arouses people's attention, such as the multi-view low-rank dictionary learning for image classification [6], the use of multi-spectral low-rank structured dictionary learning and "like charges repulsion and opposite charges attraction" law based multilinear subspace analysis for face recognition [7,8]. Nuclear norm minimization (NNM) is a low rank matrix approximation method using the F-norm and minimum nuclear norm to estimate the difference between the input and output matrices. Most low rank matrices can be well recovered by NNM. Based on NNM, weighted nuclear norm minimization (WNNM) makes an important improvement that the singular values are shrunk with different weights and more details are preserved [9]. Optimized algorithms of the WNNM are proposed successively. Du et al. proposed a joint weighted nuclear norm and total variation regularization method to denoise hyperspectral images in 2017 [10]. In this method, the Casorati matrix of hyperspectral images is a key part and the total variation regularization is imposed on each band of the hyperspectral to further remove the Gaussian noise. Another image denoising method via WNNM and Gaussian mixed model was proposed [11] and it need to use non-noise natural image blocks to train mixed Gaussian models, then perform the block matching of WNNM under the guidance of the mixed Gaussian models. However, there are no Casorati matrix, band and non-noise image in the terahertz holographic reconstructed image and it cannot be trained.

Received May 3, 2018; accepted June 25, 2018

E-mail: liqi2013@hit.edu.cn

In a word, the above two algorithms are not suitable for terahertz holographic reconstructed image denoising. Therefore, only the WNNM algorithm has been studied and compared with the results of denoising.

Compared with the WNNM algorithm, non-local mean (NLM) method [12,13] is an efficient technique for the enhancement of images corrupted by noise. It is proven to possess satisfactory denoising effect on the whole image. The block-matching 3D (BM3D) method has an outstanding effect in the denoising of visible images [14,15].

In the terahertz holographic imaging, only the occlusion and transmissive parts are included. So the grayscale of the standard image is only 0 or 255. There are quantities of pixels on the edges of target and the grayscales of them will change from 255 to 0. The complicated details of these parts are easily lost in the denoising process. So we need to protect these details as much as possible.

When denoising the terahertz holographic reconstructed image, the WNNM method preserves the details well, but the denoising effect of background noise is not satisfactory. On the contrary, the NLM algorithm can remove background noise better, but the edge of target becomes blurry. In this paper, combining the advantages of NLM and WNNM, we proposed a new method called NLM-WNNM to denoise the real terahertz holographic reconstructed image, which was corrupted by Gaussian noises. In the NLM-WNNM, we use the NLM algorithm to further process the iteration result of WNNM in order to improve the denoising effect. In addition, simulations were conducted to investigate the generalization of the proposed method.

2 Denoising methods

2.1 WNNM denoising method [9]

There is a relationship between the noise image D and the standard image A: $D = A + N$, where N is the noise. Denoising is the process of obtaining an estimated image $\hat{A}$ from the noise image D. In WNNM, when we input the noise image D, first use the block matching method to obtain the non-local similar blocks D_j And the size of the non-local similar window is $m_2 \times m_2$ in the $m_1 \times m_1$ search window. Then use Eq. (1) to estimate the non-local similar blocks $\hat{A}_j$ of the output image. Finally similar blocks $\hat{A}_j$ are aggregated into the output image $\hat{A}$.

$$\hat{A}_j = \mathrm{argmin}_{\hat{A}_j} \frac{1}{\sigma_n^2}\|D_j - \hat{A}_j\|_F^2 + \|\hat{A}_j\|_{\mathrm{K},*}, \tag{1}$$

where σ_n^2 is the noise variance of the input image D, it is used to normalize fidelity term $\|D_j - \hat{A}_j\|_F^2$. $\|\hat{A}_j\|_{\mathrm{K},*}$ is the minimum kernel norm when the weights of the similar blocks $\hat{A}_j$ are considered. When the output similar blocks $\hat{A}_j$ are low rank matrices, the solution of Eq. (1) can be estimated by processing the soft threshold of singular values. And Eq. (1) is expressed as

$$\hat{A}_j = US_K(\Sigma)V^{\mathrm{T}}, \tag{2}$$

where U, Σ and V are the matrices obtained by the singular value decomposition of similar blocks D_j, it can be expressed as: $[U,\Sigma,V] = SVD(D_j)$. $S_K(\Sigma)$ is a diagonal matrix calculated with the weights, expressed as $S_K(\Sigma)_{ii} = \max\left(\sigma_i(D_j) - k_i, 0\right)$, where $\sigma_i(D_j)$ is the ii th diagonal element of the diagonal matrix Σ and the i th singular value of similar blocks D_j. $K = k_1,k_2,...,k_i,...,k_n$ is nonnegative weight coefficient, which is inversely proportional to singular value $\sigma_i(\hat{A}_j)$ of the similar blocks $\hat{A}_j$, the equation is

$$k_i = \frac{c\sqrt{n}}{\sigma_i(\hat{A}_j) + \varepsilon}, \tag{3}$$

where c is a contant, n is the number of similar blocks in D. $\varepsilon = 10^{-16}$ is to avoid dividing by zero. $\sigma_i(\hat{A}_j)$ is the i th singular value of similar blocks $\hat{A}_j$. $\sigma_i(\hat{A}_j)$ is calculated by

$$\sigma_i(\hat{A}_j) = \sqrt{\max\left(\sigma_i^2(D_j) - n\sigma_n^2, 0\right)}. \tag{4}$$

The process of obtaining the estimated image $\hat{A}$ from the input image D is called once iteration. Multiple iterations are required unless $\hat{A}$ does not change in the WNNM. To preserve more details, the WNNM method updates the input image before each iteration starts. The updated input image not only uses the estimated image $\hat{A}$ obtained from the previous iteration but also takes into account the input image D, that is

$$D^{t+1} = \hat{A}^t + a\left(D - \hat{A}^t\right), \tag{5}$$

where $\hat{A}^t$ is the estimated image of t th iteration ($t \geqslant 0$), a is fixed feedback value of each iteration. $D - \hat{A}^t$ is the difference between the input image and the estimated image of t th iteration. The flowchart of the WNNM method is shown in Fig. 1.

The parameters that need to be set in Fig. 1 include: m_1, m_2, σ_n^2, c, a, the number of iterations T. First, find the similar blocks of the input image and perform the singular value decomposition. Then use Eqs. (2)–(4) to estimate the similar blocks of the output image and calculate the input image of each iteration by Eq. (5). Finally aggregate all the estimated similar blocks to obtain the output image. Multi-iterations are applied in the WNNM, and the input image for each iteration is related to the estimated image obtained from the previous iteration and original input image.

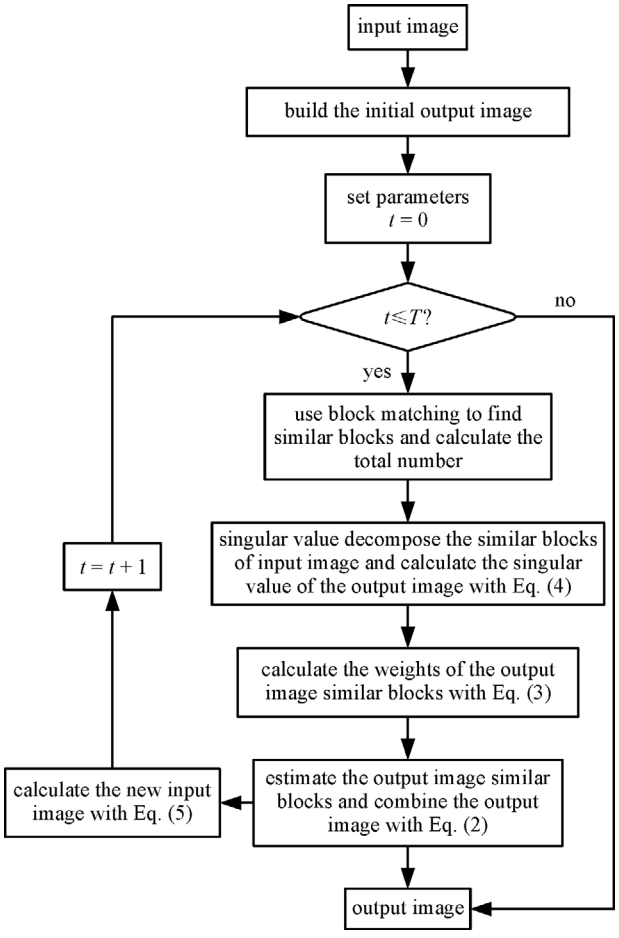

Fig. 1 Flow diagram of WNNM method

2.2 NLM method [12,13]

The NLM method estimates the gray values of the target pixels with the weighted average value in the neighborhood. Weights assigned to the pixels are determined by the similarity with the target pixel. The $NL[D]_i$ is obtained by estimating all the pixels i in the noise image D. In this process, in order to shorten the denoising time, a search window D_s with an appropriate size, instead of the whole image, is used to calculate the similarity. The equation is

$$NL[D]_i = \Sigma_{j \in D_s} w(i,j) D_j, \tag{6}$$

where $w(i,j)$ is the similarity measuring function of pixels i and j, calculated by the Euclidean distance between the gray level matrices $D(N_i)$ and $D(N_j)$. In addition, there is a limitation that $0 \leqslant w(i,j) \leqslant 1$ and $\Sigma_j w(i,j) = 1$. $w(i,j)$ is calculated by

$$w(i,j) = \frac{1}{z(i)} e^{\frac{-\|D(N_i) - D(N_j)\|_{2,a}^2}{h^2}}, \tag{7}$$

where $Z(i)$ is a normalized constant, calculated by

$$Z(i) = \Sigma_i e^{\frac{-\|D(N_i) - D(N_j)\|_{2,a}^2}{h^2}} \tag{8}$$

where $a>0$ is a standard deviation of Gaussian kernel. h acts as a filtering parameter related to the standard deviation of the input image: $h = b\sigma^2$. b is a well-chosen constant, σ is the standard deviation of the input image. From Eqs. (7) and (8), it can be seen that the weight function decreases exponentially, which indicates that the larger the Euclidean distance between two pixels, the smaller the similarity.

2.3 WNNM denoising method based on NLM algorithm (NLM-WNNM algorithm)

According to Eq. (5), the input image of the $(t+1)$ th iteration is related to the difference between the original input image D and the estimated image of the t th iteration. $D - \hat{A}^t$ includes the information of both the image details and noise, and its quality directly influences the denoising effect of WNNM algorithm. So we make the further processing to $D - \hat{A}^t$ by using NLM algorithm. In the NLM-WNNM algorithm, Eq. (5) is changed as follow:

$$D^{t+1} = \hat{A}^t + \alpha \times \mathrm{NLM}\left(D - \hat{A}^t\right), \tag{9}$$

where t is the number of iteration ($t \geqslant 0$), NLM is the NLM method. The flowchart of the NLM-WNNM method is shown in Fig. 2.

Compared with Fig. 1, the NLM algorithm is added into the process of NLM-WNNM for denoising $D - \hat{A}^t$ and Eq. (5) is replaced by Eq. (9).

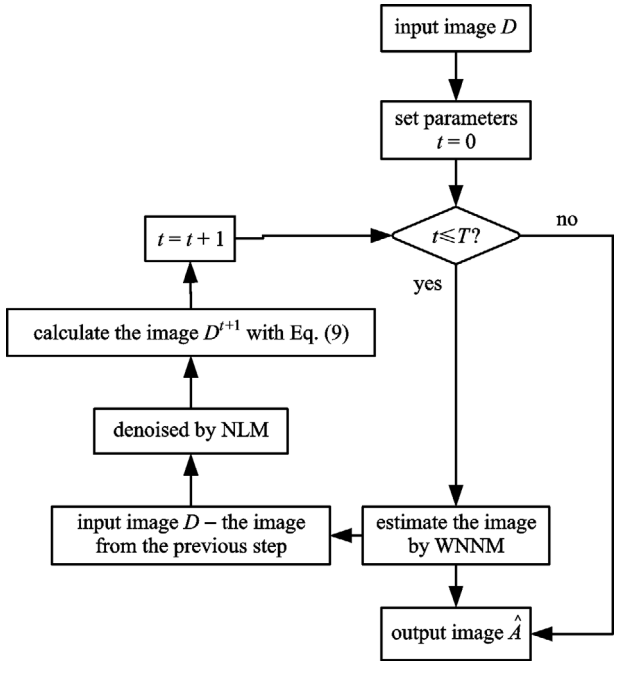

Fig. 2 Flowchart of the NLM-WNNM method

To evaluate the denoising effect quantitatively, it is necessary to calculate the peak signal to noise ratio (PSNR) and structural similarity index (SSIM) parameters. The PSNR is calculated using the following equation:

$$\mathrm{PSNR} = 10\lg\frac{255^2 M \times N}{\sum_M \sum_N (X(i,j) - Y(i,j))^2}, \tag{10}$$

where X denotes the standard image and Y is the denoising result. M,N are the number of rows and columns of the image. The mathematical expression of SSIM is

$$\mathrm{SSIM} = \frac{(2u_X u_Y + C_1)(2\sigma_{XY} + C_2)}{(u_X^2 + u_Y^2 + C_1)(\sigma_X^2 + \sigma_Y^2 + C_2)}, \tag{11}$$

where u is the mean and σ^2 is the variance. σ_{XY} is the covariance of the two images. $C_1 = (k_1 L)^2$ and $C_2 = (k_2 L)^2$, where L is the dynamic range of the pixel values. By default, $k_1 = 0.001$,$k_2 = 0.03$.

3 Experimental results and analysis

3.1 Denoising results of the terahertz holographic reconstructed image

This paper uses WNNM, NLM, BM3D and NLM-WNNM algorithm to denoise the real terahertz holographic reconstructed image with gray range of [0, 255] as Fig. 3(a) shown. It is obtained by the terahertz Gabor in-line digital holography system imaging for a gear. Parameters are as follows: in the WNNM method, the search window is 15 × 15; the standard deviation is 18; the number of iterations is 8; the feedback value is 0.69. In the NLM algorithm, the search window is 7 × 7, the similarity window is 5 × 5 and the filtering parameter h is 0.6. In the BM3D algorithm, the standard deviation is 30.

Over-filtering may occur due to the simple combination of the WNNM and NLM methods. Furthermore, the feedback processing is introduced in the 2nd iteration and the noise still accounts for a large proportion of the image at the moment. Therefore, we need to optimize the parameters of NLM-WNNM method. The filtering parameter of NLM-WNNM is 0.7. However, as the number of iterations increases, the proportion of noise in the image gradually decreases. So the parameters should be changed again. The new filter parameter and feedback value are set as 0.3 and 0.5. The real terahertz holographic reconstructed image, the standard image, the histogram of the object regions in the real image and the denoising results of WNNM, NLM, BM3D and NLM-WNNM are shown in Fig. 3. It is difficult to compare these methods because there are many uniform regions in the image in which the gray values are all 255. The PSNR and SSIM results of the object regions are listed in Table 1.

Comparing the results shown in Fig. 3 and Table 1, the noise in the image is closest to the Gaussian noise according to Fig. 3(c). In Fig. 3(d), the WNNM method preserves the details of the “gear” well, but there is still obvious noise in the background. In Fig. 3(e), after

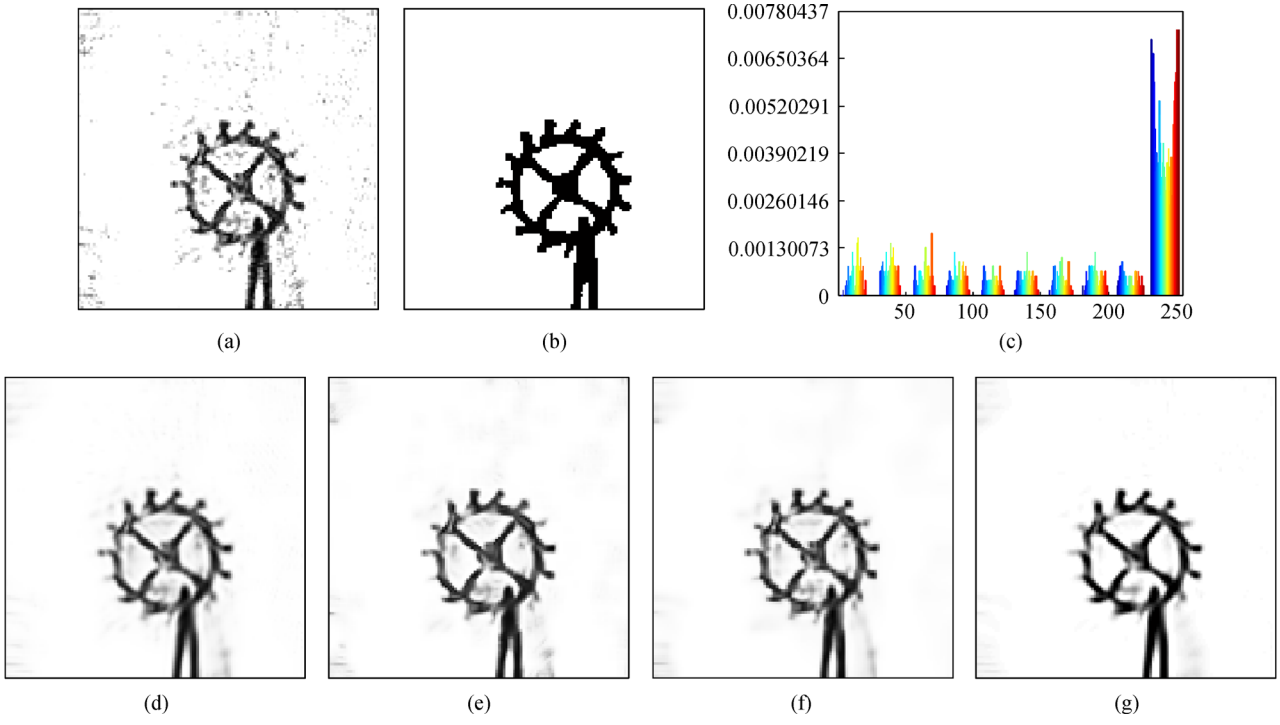

Fig. 3 Terahertz holographic reconstructed images. (a) Real image; (b) standard image; (c) histogram of the object regions in real image; (d) denoised by WNNM; (e) denoised by NLM; (f) denoised by BM3D; (g) denoised by NLM-WNNM

Table 1 PSNR and SSIM of terahertz image before and after denoised

method	PSNR	SSIM
real image	64.52	0.7662
WNNM	64.90	0.8779
NLM	64.88	0.8789
BM3D	64.85	0.8812
NLM-WNNM	65.15	0.8866

denoised by NLM, most of the background noise is removed. However, some details of the "gear" are lost. In Fig. 3(f), there is some noise in the internal of the "gear" and the result is similar to that of NLM method. The reason is that these two methods use the same way to find the paths, and it is difficult to find the suitable paths in the internal of the "gear." So the internal noise is maintained and regarded as the details of input image. In contrast, in the NLM-WNNM method, there are more similar paths in the difference image of the original input image and the output image in each iteration, then the NLM method is used to denoise the difference image. So it is easier to remove the noise. As shown in Fig. 3(g), when the denoising is performed using NLM-WNNM, the noise in the background is well eliminated and the shape of the "gear" remains unaffected. In addition, this new method has the largest PSNR and SSIM, which is consistent with the subjective evaluation. Therefore, the new method we proposed is proven to provide a better denoising of the real terahertz holographic reconstructed image.

3.2 Denoising results of visible image

To verify the generalization of the NLM-WNNM algorithm, it was applied to denoise the visible images. Zero mean additive white Gaussian noise with variance 0.01 are added to the visible image to generate the noise image. The size of the Lena image is 512×512 and the gray range is [0,255]. Parameters are as follows. In the WNNM method, the number of iterations is 14, the feedback value is 0.71. In the NLM algorithm, the search window is 21×21, the similarity window is 7×7 and the filtering parameter h is 0.41 [8]. The parameters of the proposed method are as follows. The number of iterations is 16, the filtering parameter h is 0.45, and other parameters in the NLM-WNNM are the same as those of the above two algorithms. The parameters of BM3D are default. The noise image, the standard image and the denoising results of WNNM, NLM, BM3D and NLM-WNNM are shown in Fig. 4. The PSNR and SSIM results are listed in Table 2.

As shown in Table 2, it can be seen that the NLM-WNNM method outperforms the NLM and WNNM methods with the largest PSNR and SSIM when dealing with Lena image. The performance of BM3D method is best, because the Lena image is different from the terahertz holographic reconstructed image, its gray is from 0 to 255 instead of only 0 and 255. For the whole image, it is easy to correctly find the similar paths and set the threshold in the 3D transformation before the collaborative filtering. And we can also see that the BM3D method is much better than the WNNM and NLM methods, so it is acceptable that the

Fig. 4 Lena images. (a) Noise image; (b) standard image; (c) denoised by WNNM; (d) denoised by NLM; (e) denoised by NLM-WNNM; (f) denoised by BM3D

Table 2 PSNR and SSIM of the Lena image before and after denoised

method	PSNR	SSIM
noise image	68.20	0.6188
WNNM	78.43	0.9021
NLM	78.34	0.8944
NLM-WNNM	78.81	0.9132
BM3D	80.10	0.9261

NLM-WNNM is not better than BM3D when denoising Lena image.

However, it is difficult to visually evaluate the denoising effect of WNNM, NLM, BM3D and NLM-WNNM from the complicated details in Fig. 4. To make a clear comparison, we choose parts of the image for comparison and analysis. In the "hair" area, the region has a high resolution and the change of grayscale is complicated. The comparison results are shown in Fig. 5.

The selected area is marked by the cross in Fig. 5(a). As shown in Figs. 5(b) and 5(c), in most areas, the gray values after denoised by NLM-WNNM are closest to those of standard image. It is evident that this new method performs best when dealing with images where the change of grayscales is complicated. And the situation is similar to the "gear" in the terahertz holographic reconstructed image.

The "eyeball" area in the Lena image mainly contains uniform areas with a gradual change of grayscales. The comparison results are shown in Fig. 6.

The selected area is marked by the cross in Fig. 6(a). As shown in Figs. 6(b) and 6(c), in uniform areas, the gray values after denoised by BM3D are closest to those of the standard image, followed by NLM, NLM-WNNM and WNNM. We can draw a conclusion that the BM3D has the best denoising effect when dealing with images where the change of grayscales is uniform, and the NLM-WNNM does not have a better performance. Considering the above results gained from Figs. 5 and 6, the NLM-WNNM method is more suitable for the denoising of images with complicated details and high resolution.

4 Conclusion

This paper proposed a new method called NLM-WNNM

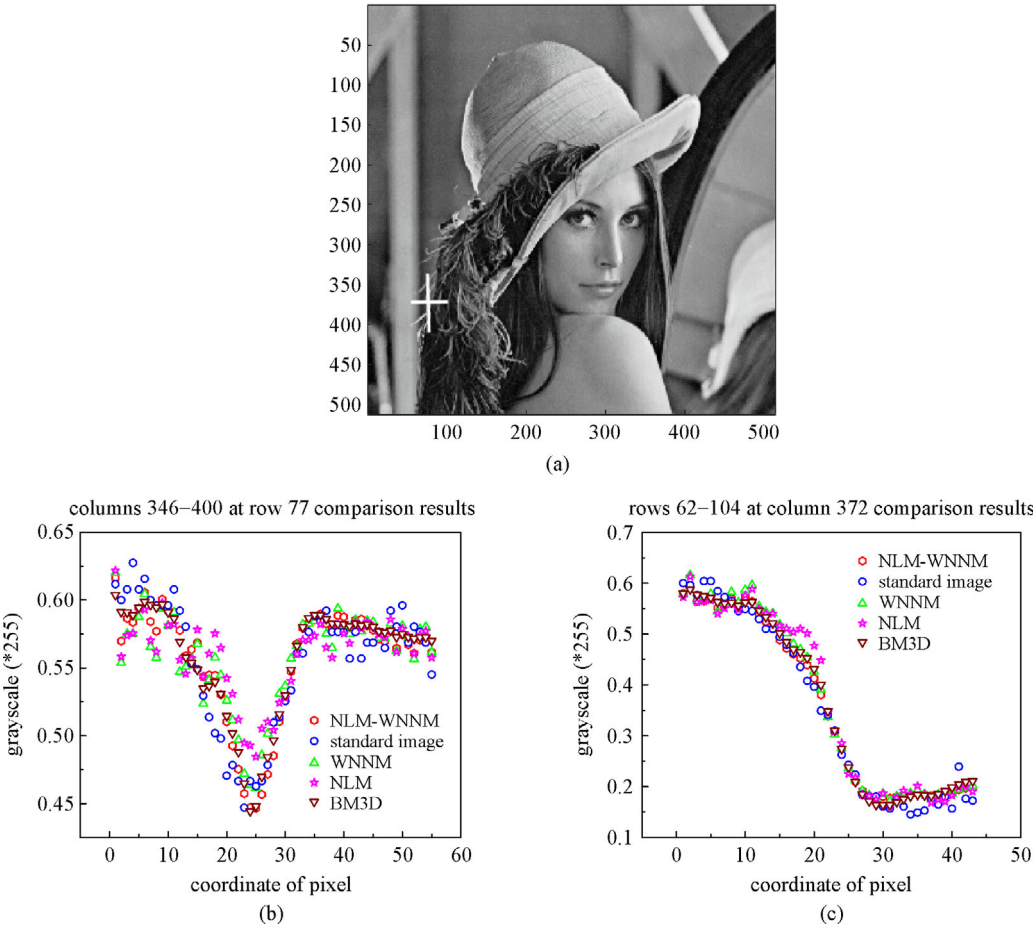

Fig. 5 Comparison results. (a) Selected "hair" area; (b) columns 346 –400 at row 77 comparison results; (c) rows 62 –104 at column 372 comparison results

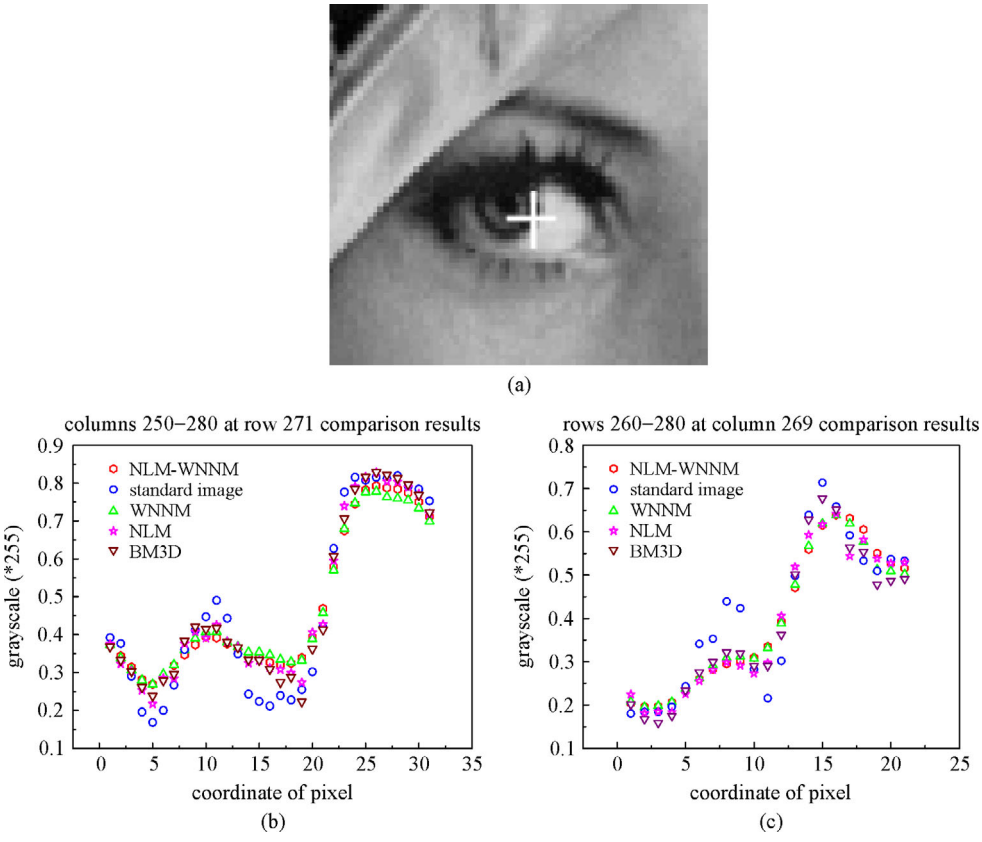

Fig. 6 Comparison results. (a) Selected "eyeball" area; (b) columns 250–280 at row 271 comparison results; (c) rows 260–280 at column 269 comparison results

combining the advantages of WNNM and NLM algorithm. Experimental results show that the NLM-WNNM method has the best performance when applied to denoise the terahertz Gabor in-line digital holography holographic reconstructed image. However, when dealing with visible images, though the new method is not better than BM3D, it has a better denoising result compared with the original methods. Simulation experiment results confirm that the NLM-WNNM algorithm is promising in the denoising of images with complicated details and high resolution.

Acknowledgements This work was supported by the National Natural Science Foundation of China (NSFC) (Grant No. 61377110).

References

1. Zheng X, Wang X, Sun W,Feng S, Ye J, Zhang Y.Developments and applications of the terahertz digital holography. Chinese Journal of Lasers, 2014, 41(2): 1–11
2. Wang D, Huang H, Zhou X, Rong L, Li Z, Lin Q, Wang Y. Phase-contrast Imaging by the continuous-wave terahertz in-line digital holography. Chinese Journal of Lasers, 2014, 41(8): 08090031–08090036
3. Xue K, Li Q, Li Y D, Wang Q. Continuous-wave terahertz in-line digital holography. Optics Letters, 2012, 37(15): 3228–3230
4. Cui S S, Li Q. A comparison of filtering techniques on denoising terahertz coaxial digital holography image. SPIE, 2016, 10157: 101571R1–101571R5
5. Cui S, Li Q. Denoising research on terahertz digital holography based on wavelet transform. Infrared and Laser Engineering, 2015, 44(6): 1836–1840
6. Wu F, Jing X Y, You X, Yue D, Hu R, Yang J Y. Multi-view low-rank dictionary learning for image classification. Pattern Recognition, 2016, 50: 143–154
7. Jing X Y, Wu F, Zhu X, Dong X, Ma F, Li Z. Multi-spectral low-rank structured dictionary learning for face recognition. Pattern Recognition, 2016, 59: 14–25
8. Wu F, Jing X Y, Wu S, Gao G, Ge Q, Wang R. "Like charges repulsion and opposite charges attraction" law based multilinear subspace analysis for face recognition. Knowledge-Based Systems, 2018, 149: 76–87
9. Gu S H, Zhang L,Zuo W M,Feng X C. Weighted nuclear norm minimization with application to image denoising. In: Proceedings of IEEE Conference on Computer Vision and Pattern Recognition (CVPR). Columbus, OH, USA: IEEE, 2014, 2862–2869
10. Du B, Huang Z, Wang N, Zhang Y, Jia X. Joint weighted nuclear norm and total variation regularization for hyperspectral image denoising. International Journal of Remote Sensing, 2018, 39(2): 334–355

11. Sun S. Image denoising via weighted nuclear norm minimization and Gaussian mixed model. Jisuanji Yingyong, 2017, 37(5): 1471–1474
12. Buades A, Bartomeu C A, Morel J M. A non-local algorithm for image denoising. In: Proceedings of IEEE Computer Society Conference on Computer Vision and Pattern Recognition (CVPR). San Diego, CA, USA: IEEE, 2005, 61–65
13. Buades A, Bartomeu C A, Morel J M. Non-local means denoising. IPOL Journal—Image Processing on Line, 2011, 1: 208–212
14. Dabov K, Foi A, Katkovnik V, Egiazarian K. Image denoising by sparse 3-D transform-domain collaborative filtering. IEEE Transactions on Image Processing, 2007, 16(8): 2080–2095
15. Image and video denoising by sparse 3D transform-domain collaborative filtering, http://www.cs.tut.fi/~foi/GCF-BM3D; GitHub, https://github.com/glemaitre/BM3D

Wenshu Ma,student in Harbin Institute of Technology. Her current research is Terahertz image processing.
E-mail: hit_mawenshu@163.com

Qi Li, professor in Harbin Institute of Technology. Her research interests focus on laser and terahertz imaging and image processing. She has won the third prize of Science and Technology Progress in Natural Science in Heilongjiang Province.
E-mail: liqi2013@hit.edu.cn

Jianye Lu, associate professor in Harbin Institute of Technology. His research interests focus on laser technology and image processing.
E-mail: lujy@hit.edu.cn

Liyu Sun, master in Harbin Institute of Technology. His current research is image information processing.